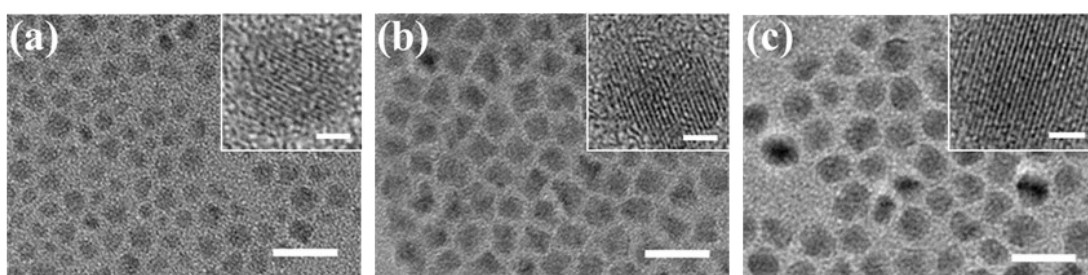


## Quantum-dots-encapsulated core-shell barcodes from droplet microfluidics

Feika Bian, Huan Wang, Lingyu Sun, Yuxiao Liu, Yuanjin Zhao\*

State Key Laboratory of Bioelectronics, School of Biological Science and Medical  
Engineering, Southeast University, Nanjing 210096, China

Email: yjzhao@seu.edu.cn



**Fig. S1** TEM image of (a) QD<sup>448</sup>, (b) QD<sup>513</sup> and (c) QD<sup>626</sup>. The scale bar indicates 20 nm and 2nm in illustration.

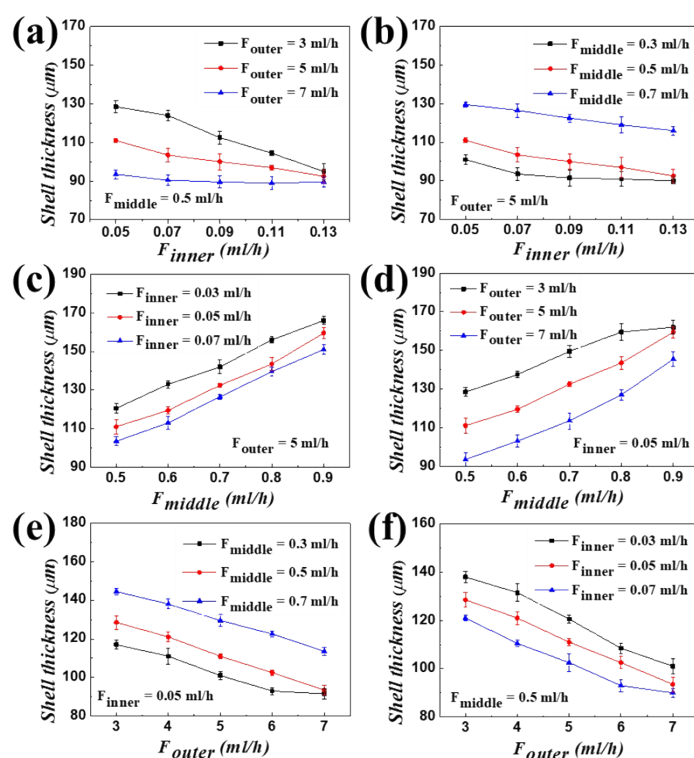


**Fig. S2 (a-f)** The shell thickness of the drops decreased with  $F_{\text{inner}}$  and  $F_{\text{outer}}$ , while increased with  $F_{\text{middle}}$ . It was also found that when the value of  $F_{\text{outer}}$  was kept constant and  $F_{\text{inner}}/F_{\text{middle}}$  was changed,  $R_{\text{out}}$  showed no regular changes, and when adjusting the ratio of  $F_{\text{inner}}$  to  $F_{\text{middle}}$ , none of these parameters ( $F_{\text{inner}}$ ,  $F_{\text{middle}}$ ,  $F_{\text{inner}}+F_{\text{middle}}$ ) was fixed.

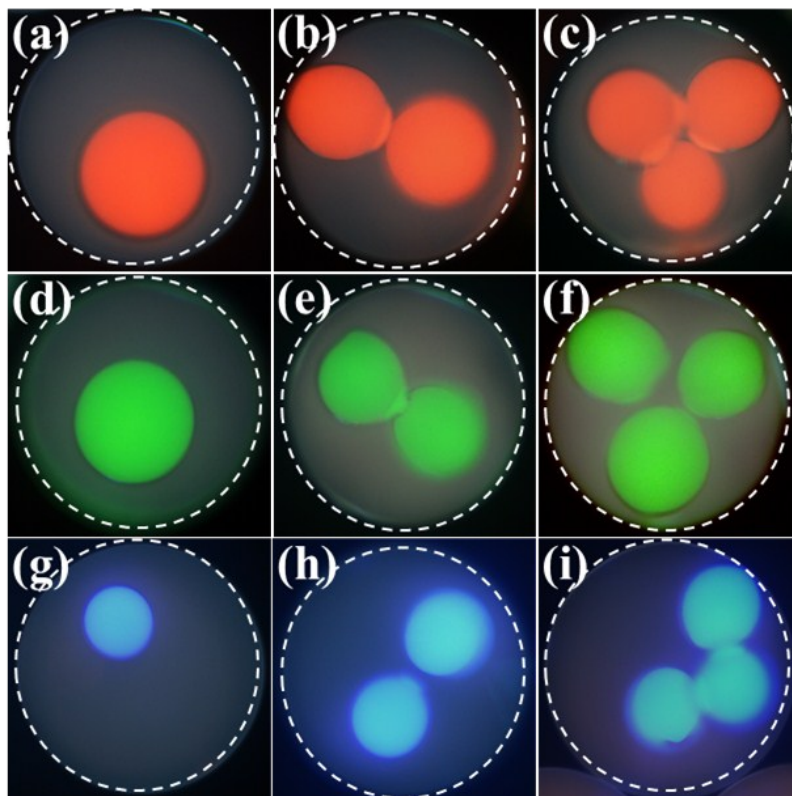


**Fig. S3** The fluorescent microscope images of QDs-encapsulated core-shell barcodes with (a-c) red QDs, (d-f) green QDs and (g-i) blue QDs.

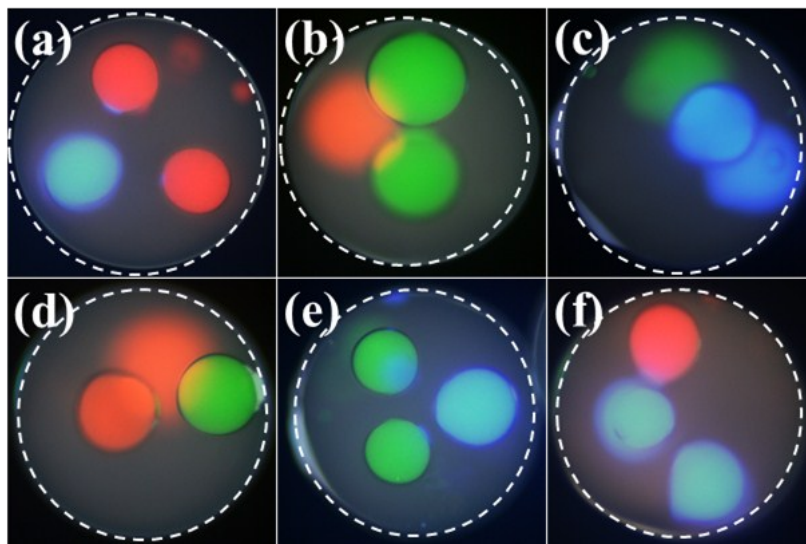


**Fig. S4** The fluorescent microscope images of QDs-encapsulated core-shell barcodes with two QDs types. (a) barcode 1:0:2, (b) barcode 0:2:1, (c) barcode 2:1:0, (d) barcode 0:1:2, (e) barcode 0:2:1, (f) barcode 2:0:1 .

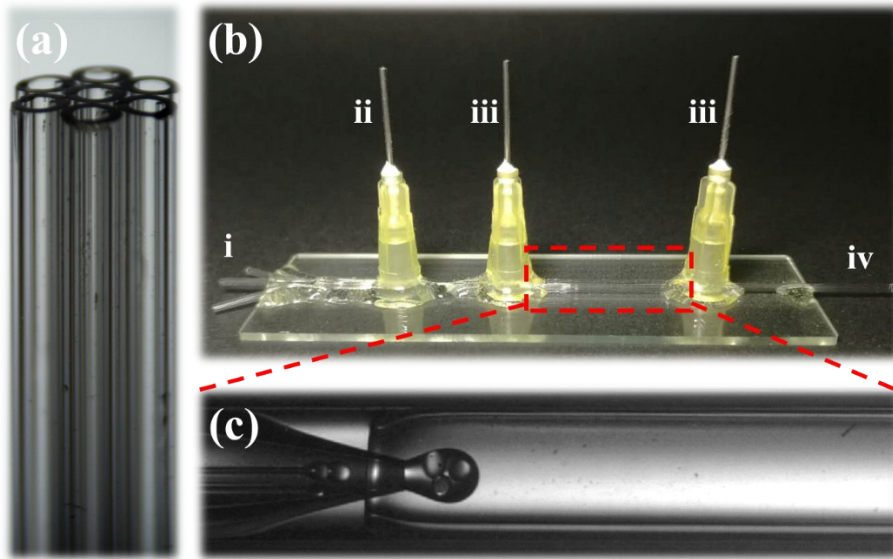


**Fig. S5** (a) a microscopy photograph of the seven-bore annular capillary; (b) a digital photograph of the assembled capillary microfluidic device, i–iv are the inner, middle, outer and collection channels, respectively. (c) a real-time generation photograph of microfluidics.

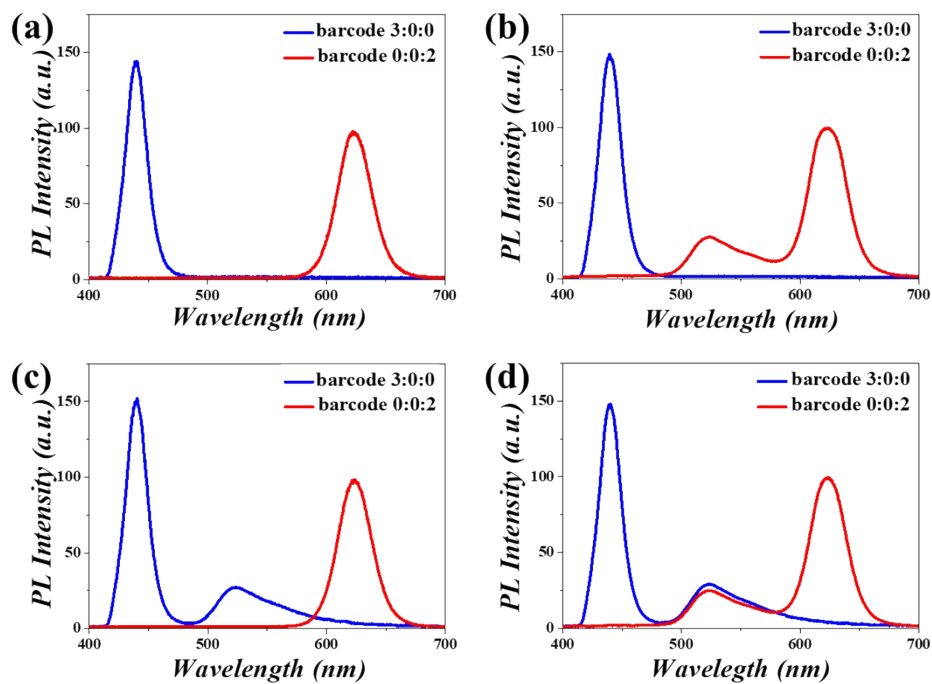


**Fig. S6** The fluorescence spectrum of rabbit IgG and human IgG detection by fibre spectrometer, (a) no target antigen existed, (b) only human IgG existed, (c) only human IgG existed and (d) both of two antigen existed.